^{18}F-fluoromisonidazole positron emission tomography may differentiate glioblastoma multiforme from less malignant gliomas

Running Title: FMISO PET for Glioma Grading

Kenji Hirata[1]; Shunsuke Terasaka[2]; Tohru Shiga[1]; Naoya Hattori[3]; Keiichi Magota[4]; Hiroyuki Kobayashi[2]; Shigeru Yamaguchi[2]; Kiyohiro Houkin[2]; Shinya Tanaka[5]; Yuji Kuge[6]; and Nagara Tamaki[1]

[1]Department of Nuclear Medicine, Hokkaido University Graduate School of Medicine, Sapporo, Japan
[2]Department of Neurosurgery, Hokkaido University Graduate School of Medicine, Sapporo, Japan
[3]Department of Molecular Imaging, Hokkaido University Graduate School of Medicine, Sapporo, Japan
[4]Department of Radiology, Hokkaido University Hospital, Sapporo, Japan
[5]Department of Cancer Pathology, Hokkaido University Graduate School of Medicine, Sapporo, Japan
[6]Central Institute of Isotope Science, Hokkaido University, Sapporo, Japan

Type of article: Original article
Source of Funding:
(1) Special Coordination Funds for Promoting Science and Technology of the Ministry of Education, Culture, Sports, Science and Technology of Japan.
(2) Grant-in-Aid for General Scientific Research from the Japan Society for the Promotion of Science.

Corresponding author & First author:
Kenji Hirata, M.D., Ph.D
Clinical Fellow
Department of Nuclear Medicine, Graduate School of Medicine, Hokkaido University
Kita 15, Nishi 7, Kita-Ku, Sapporo, Hokkaido, JAPAN 060-8638
TEL: +81-11-706-5152 FAX: +81-11-706-7155
E-mail address: khirata@med.hokudai.ac.jp

Total word count: 5768 words

Abstract

Glioblastoma multiforme (GBM) is the most aggressive primary brain tumor and its prognosis is significantly poorer than those of less malignant gliomas. Pathologically, necrosis is one of the most important characteristics that differentiate GBM from lower grade gliomas; therefore, we hypothesized that ^{18}F fluoromisonidazole (FMISO), a radiotracer for hypoxia imaging, accumulates in GBM but not in lower grade gliomas. We aimed to evaluate the diagnostic value of FMISO PET for the differential diagnosis of GBM from lower grade gliomas. *Methods*: This prospective study included 23 patients with pathologically confirmed gliomas. All the patients underwent FMISO PET and FDG PET within a week. FMISO images were acquired 4 hours after intravenous administration of 400 MBq of FMISO. Tracer uptake in the tumor was visually assessed. Lesion-to-normal tissue ratios and FMISO uptake volume were calculated. *Results*: Thirteen of the 23 glioma patients were diagnosed as having GBM (grade IV glioma in WHO classification 2007), and the others were diagnosed as having non-GBM (5 grade III and 4 grade II). In visual assessment, all the GBM patients showed FMISO uptake in the tumor greater than that in the surrounding brain tissues, whereas all the non-GBM patients showed FMISO uptake in the tumor equal to that in the surrounding brain tissues (p<0.001). One GBM patient was excluded

from FDG PET study because of hyperglycemia. All the GBM patients and 3 of the 9 (33 %) non-GBM patients showed FDG uptake greater than or equal to that in the gray matter. The sensitivity and specificity for diagnosing GBM were 100 % and 100 % for FMISO, and 100 % and 66 % for FDG, respectively. The lesion-to-cerebellum ratio of FMISO uptake was higher in GBM patients (2.74±0.60, range: 1.71 - 3.81) than in non-GBM patients (1.22±0.06, range: 1.09 - 1.29, $p<0.001$) with no overlap between the groups. The lesion-to-gray matter ratio of FDG was also higher in GBM patients (1.46±0.75, range: 0.91 – 3.79) than in non-GBM patients (1.07±0.62, range: 0.66 – 2.95, $p<0.05$); however, overlap of the ranges did not allow clear differentiation between GBM and non-GBM. Uptake volume of FMISO was larger in GBM (27.18±10.46 %, range: 14.02 - 46.67 %) than in non-GBM (6.07±2.50 %, range: 2.12 - 9.22 %, $p<0.001$). *Conclusion*: These preliminary data suggest that FMISO PET may distinguish GBM from lower grade gliomas.

Key words: glioblastoma multiforme; hypoxia; fluoromisonidazole; fluorodeoxyglucose

Introduction

Glioblastoma multiforme (GBM) is the most aggressive astrocytic tumor of cerebral gliomas, which is categorized as grade IV in WHO classification [1]. Although surgery, radiotherapy, and chemotherapy can improve the prognosis [2], a recent comparative study showed that the one-year survival rate of GBM patients is 56 %, which is significantly poorer than those with grade III (78 %) or less malignant gliomas [3]. Therefore, grading of malignancy will provide accurate prognosis information and allow us to determine the best therapy [1, 4].

Surgical biopsy or resection followed by pathological exploration is necessary to confirm the diagnosis of GBM [4]. However, craniotomy, particularly surgery of eloquent regions, can involve surrounding brain tissues, and can exacerbate prognosis by causing neurological morbidity [5]. In addition, the effect of tumor resection on prognosis remains controversial [2, 6, 7], whereas the universally accepted favorable prognosis factors are young age and good performance status only [2, 4].

In vivo imaging modalities including magnetic resonance (MR) imaging and positron emission tomography (PET) using ^{18}F fluorodeoxyglucose (FDG) play important roles in the diagnosis of GBM. A ring-like enhancement by gadolinium on

MR images and an intense uptake of FDG suggest GBM [4, 8-15]. However, not all GBM patients show a ring-like enhancement, resulting in false negative diagnosis [4]. In addition, FDG uptake frequently causes a false positive outcome owing to a significant number of patients of grade III glioma with high FDG uptake [13, 14]. The inaccuracy of these modalities restricts the omission of biopsy. Thus, the establishment of new, noninvasive, and more accurate imaging for glioma grading is required in clinical settings [11].

Histopathologically, GBM tissue includes microvascular proliferation and necrosis as well as anaplasia and mitotic activity, while necrotic tissues do not exist in grade III or lower grade gliomas, as defined by WHO [1]. GBM is exposed to severe hypoxia and therefore necrotic tissues are developed, whereas grade III or lower grade gliomas survive in less hypoxic conditions [16-19]. Therefore, imaging of hypoxia in GBM may provide important information to distinguish GBM from less malignant gliomas.

^{18}F-fluoromisonidazole (FMISO) is a radiotracer that can be used to identify regional hypoxia in vivo [20-22]. Since Valk et al. introduced the use of FMISO for glioma imaging [23], it has been intensively investigated by many researchers [24-30]. While they agree that FMISO accumulates in GBM, few data are available about

FMISO accumulation in grade III or less malignant gliomas, although a paper showed no uptake of FMISO in grade II gliomas [26]. We hypothesized that FMISO accumulates in GBM but not in lower grade gliomas and that hypoxia imaging using FMISO can accurately discriminate GBM from lower grade gliomas. Thus, the purpose of this study was to evaluate the diagnostic value of FMISO PET in glioma grading in comparison with that of FDG PET in patients suspected of having GBM on MR images.

Materials and Methods

Patients

Twenty-seven patients with possible high-grade glioma were prospectively studied according to the criteria that the patient presents with cerebral parenchymal tumor surrounded by edematous tissues on MR images but without a known malignancy in other organs. No previous tumorectomy, chemotherapy, or radiotherapy for the lesion was performed except for a patient who showed tumor recurrence 6 years after she underwent tumorectomy followed by chemoradiotherapy for low grade glioma. Two patients were excluded because of contraindication of surgical operations. The

remaining 25 patients underwent tumoral resection (n=16) or biopsy (n=9) at most 2 weeks after the PET scanning. Pathological diagnosis based on WHO classification was determined by two experienced neuropathologists by agreement. The images of MR imaging and PET were not given to the neuropathologists. Two patients, diagnosed as having metastatic adenocarcinoma and multiple sclerosis, respectively, were excluded from this study. Therefore, the final analyzed population consisted of 23 patients (M:F=10:13, age 57.0±15.2 years old) with pathologically confirmed gliomas. Maximum diameter of the tumor was measured on fluid attenuated inversion recovery (FLAIR) MR images for each patient. Intensity of gadolinium enhancement was determined by an experienced radiologist. Maximum diameter of gadolinium-enhanced area was measured when the patient showed positive enhancement. The Ethics Committee of Hokkaido University Hospital approved the study. Written informed consent was obtained from all the patients included in this study.

PET protocol

All the patients underwent the same protocol of PET acquisition using FMISO and FDG within a week. FMISO was synthesized using the previously described protocol [31, 32]. Four hours after the intravenous injection of 400 MBq of FMISO,

static PET images of the brain were acquired. On another day, following blood glucose test, 400 MBq of FDG was intravenously injected and one hour later the brain was scanned. All the images were acquired using a high-resolution PET scanner (ECAT HR+ scanner; Asahi-Siemens Medical Technologies Ltd., Tokyo, Japan) operated in a three-dimensional mode, except that the FMISO images of patient No. 23 were acquired using an integrated PET-CT scanner (Biograph 64 PET-CT scanner; Asahi-Siemens Medical Technologies Ltd., Tokyo, Japan). The image acquisition using the ECAT HR+ scanner consisted of 10 minutes of emission scanning and 3 minutes of transmission scanning with a $^{68}Ge/^{68}Ga$ retractable line source. The same acquisition protocol was used for FMISO and FDG. For the Biograph 64 PET-CT scanner, 10 minutes of emission scanning was carried out and CT images were acquired for attenuation corrections. Attenuation-corrected radioactivity images for both scanners were reconstructed using a filtered backprojection with a Hann filter of 4 mm full width at half maximum.

Visual assessment

In the visual assessment of FMISO PET results, first, FMISO uptake was visually divided into 3 categories. When the highest intratumoral uptake was less than

that in the surrounding brain tissue, the patient was considered as showing *low FMISO uptake*. When the highest intratumoral uptake was equal to that in the surrounding brain tissue, the patient was considered as showing *intermediate FMISO uptake*. When the highest intratumoral uptake was greater than that in the surrounding brain tissue, the patient was considered as showing *high FMISO uptake*. Next, patients showing *low FMISO uptake* and *intermediate FMISO uptake* were grouped together as FMISO-negative patients, whereas those showing *high FMISO uptake* were defined as FMISO-positive patients [26].

In the visual assessment of FDG PET results, we evaluated FDG accumulation in the tumor on the basis of a previously reported assessment system [14]. First, FDG uptake was visually divided into 3 categories. When the highest intratumoral uptake was less than or equal to that in the contralateral white matter, the patient was considered as showing *low FDG uptake*. When the highest intratumoral uptake was greater than that in the contralateral white matter and less than that in the contralateral gray matter, the patient was considered as showing *intermediate FDG uptake*. When the highest intratumoral uptake was equal to or greater than that in the contralateral gray matter, the patient was considered as showing *high FDG uptake*. Next, patients showing *low FDG uptake* and *intermediate FDG uptake* were grouped together as FDG-negative patients,

whereas those showing *high FDG uptake* were defined as being FDG-positive patients. An experienced nuclear physician who did not know pathological diagnosis visually evaluated all the images.

Standardized uptake values and lesion-to-normal tissue ratios

PET images were anatomically coregistered with individual FLAIR MR images using a mutual information algorithm implemented in NEUROSTAT software package [33, 34]. First, polygonal regions of interest (ROI) were manually drawn to enclose peritumoral edematous regions as well as tumoral regions on every slice. FLAIR and gadolinium enhanced images were both considered to determine ROI. The single voxel with highest radioactivity concentration in the tumor was automatically detected in the PET images. And then, the highest radioactivity was converted into standardized uptake value (SUV), and was defined as SUV_{max}. A circular ROI (10 mm in diameter) whose center was located on the maximum voxel was automatically created. The voxels in the circular ROI were averaged as SUV_{10mm}. SUV was calculated as (tissue radioactivity [Bq/ml])*(body weight [g]) / (injected radioactivity [Bq]). Next, the following reference regions were identified on the FLAIR images on each patient: (1) cerebellar cortex, (2) contralateral frontoparietal cortex on the level of centrum

semiovale, and (3) contralateral frontoparietal white matter on the level of centrum semiovale. Multiple uniform ROIs, each with a circular shape and of 10 mm diameter, were placed in the manner described as follows; first, 15 ROIs (5 ROIs on each of the 3 axial slices) were placed on both sides of the cerebellar cortex. FMISO counts of a total of 30 ROIs on the cerebellum were averaged. The lesion-to-cerebellum ratio of FMISO was calculated by dividing SUV_{10mm} by cerebellar averaged SUV. Then, we placed 15 ROIs (5 ROIs on each of the 3 axial slices) on the contralateral frontoparietal cortex, and 5 ROIs (5 ROIs on the one axial slice) on contralateral frontoparietal white matter. FDG counts of ROIs on the contralateral frontoparietal cortex and white matter were averaged. The lesion-to-gray matter and lesion-to-white matter ratios of FDG were calculated by dividing SUV_{10mm} by gray matter and white matter averaged SUV, respectively [13]. An experienced nuclear physician placed all the ROIs. When a tumor occupied bilateral lobes, the hemisphere where the larger part of the tumor existed was defined as the side of the tumor.

FMISO uptake volume

We measured the tissue volume showing significant FMISO uptake in the tumor compared to cerebellum. The voxels having higher SUV than 1.3-fold cerebellar

mean SUV were extracted in the tumoral ROI described above. The value of 1.3 was used for image segmentation in ^{11}C methionine brain PET [30, 35, 36]. The FMISO uptake volume was expressed as a percentage of the extracted voxels in the whole tumoral ROI.

Statistical analysis

All parametrical data were expressed as mean ± SD. All the patients with grade III or less malignant gliomas were grouped together as non-GBM patients to simplify the analysis. The association between histopathological diagnosis and visual assessment results was examined using Fisher's exact test. The differences in age, tumor size, SUVs, lesion-to-normal tissue ratios, and uptake volume between GBM and non-GBM patients were examined using Mann-Whitney U-test. *P*-values less than 0.05 were considered statistically significant. R 2.14.0 for Windows was used for statistical analysis and figure drawing.

Results

Pathological diagnosis and MR imaging

Table 1 summarizes the patients' characteristics, pathological diagnoses, and MR imaging results. Fourteen patients were diagnosed as having GBM and therefore categorized as grade IV in WHO classification. Five patients were diagnosed as having grade III gliomas, consisting of 1 anaplastic astrocytoma, 1 anaplastic oligodendroglioma, and 3 anaplastic oligoastrocytomas. The patient with recurrent glioma (n=1, No. 15) was diagnosed as anaplastic astrocytoma. Four patients were diagnosed as having grade II gliomas, consisting of 1 diffuse astrocytoma, 1 oligodendroglioma, and 2 oligoastrocytoma. A total of 9 patients categorized as grade II or grade III were grouped together as non-GBM. Pathologically, regional necrosis was found in all the GBM patients, whereas none of non-GBM patients showed necrosis in the tumor. The average age of GBM patients was 65.5±9.9 years, which was significantly older than that of non-GBM patients (43.7±12.2 years, $p<0.01$). The maximum diameter measured on FLAIR MR images was not significantly different between GBM (64.4±17.5 mm) and non-GBM (77.6±22.5 mm, $p=0.37$) patients. Three of 9 non-GBM patients did not show gadolinium enhancement in the tumor, whereas all

the GBM patients showed gadolinium enhancement in the tumor. The maximum diameter of enhanced area was not significantly different between GBM (42.3±12.9 mm, n=14) and non-GBM (36.4±14.3 mm, n=6, p=0.44) patients.

Visual assessment

PET results of each patient were shown in Table 2. In all the GBM patients (14/14), FMISO uptake in the tumor was greater than that in the surrounding brain tissues (*high FMISO uptake*, Fig. 1c). On the other hand, all the non-GBM patients (9/9) showed FMISO uptake equal to that in the surrounding brain tissues (*intermediate FMISO uptake*, Fig. 2c, 3c). No patient showed FMISO uptake less than that in the surrounding brain tissues (*low FMISO uptake*). As a result, 14 patients showed GBM and FMISO-positive, no patient showed GBM and FMISO-negative, no patient showed non-GBM and FMISO-positive, and 9 patients showed non-GBM and FMISO-negative. A significant association was observed between histology (GBM or non-GBM) and FMISO uptake (FMISO-positive or FMISO-negative) (p<0.001). Visual assessment of FMISO PET images predicted GBM with sensitivity, specificity, and accuracy of 100 %, 100 %, and 100 %, respectively.

A patient (No. 13) showed hyperglycemia due to diabetes mellitus. No other

patients showed fasting blood sugar level higher than 150 mg/dl. Since FDG PET may be affected by hyperglycemia, we excluded the diabetic patient from all the analyses of FDG PET. All the GBM patients showed FDG uptake greater than that in the contralateral gray matter (*high FDG uptake*, Fig. 1d). *High FDG uptake*, *intermediate FDG uptake*, and *low FDG uptake* were observed in 3 (33 %, Fig. 2d), 3 (33 %, Fig. 3d), and 3 (33 %) of the 9 non-GBM patients, respectively. As a result, 13 patients showed GBM and FDG-positive, no patient showed GBM and FDG-negative, 3 patients showed non-GBM and FDG-positive, and 6 patients showed non-GBM and FDG-negative. The association between histology (GBM or non-GBM) and FDG uptake (FDG-positive or FDG-negative) reached statistical significance ($p<0.01$). Visual assessment of FDG PET images predicted GBM with sensitivity, specificity, and accuracy of 100 %, 66 %, and 86 %, respectively.

Standardized uptake values and lesion-to-normal tissue ratio analysis

SUV_{max} of FMISO was higher in GBM patients (3.09±0.62, range: 2.22 - 4.31) than in non-GBM patients (1.73±0.36, range: 1.36 - 2.39, $p<0.001$). SUV_{10mm} of FMISO was higher in GBM patients (3.00±0.61, range: 2.15 - 4.18) than in non-GBM patients (1.64±0.38, range: 1.29 - 2.35, $p<0.001$). The lesion-to-cerebellum ratio of FMISO,

calculated by dividing SUV_{10mm} by cerebellar averaged SUV, was higher in GBM patients (2.74±0.60, range: 1.71 - 3.81) in GBM patients than in non-GBM patients (1.22±0.06, range: 1.09 - 1.29, $p<0.001$, Fig. 4a).

The diabetic patient was excluded from SUV and lesion-to-normal tissue ratio analyses of FDG PET. SUV_{max} of FDG did not significantly differ between GBM (7.55±3.72, range: 4.34 - 16.38) and non-GBM (8.21±6.04, range: 4.75 - 23.49, $p=0.95$). SUV_{10mm} of FDG did not significantly differ between GBM (7.41±3.63, range: 4.26 - 15.90) and non-GBM (8.03±5.96, range: 4.64 - 23.12, $p=0.95$). On the other hand, the lesion-to-gray matter ratio of FDG, calculated by dividing SUV_{10mm} by averaged SUV in the contralateral gray matter, was higher in GBM patients (1.46±0.75, range: 0.91 - 3.79) than in non-GBM patients (1.07±0.62, range: 0.66 - 2.95, $p<0.05$, Fig. 4a). The lesion-to-white matter ratio of FDG, calculated by dividing SUV_{10mm} by averaged SUV in the contralateral white matter, did not reach statistical significance between GBM (2.81±1.23, range: 1.87 - 6.44) and non-GBM (2.66±1.60, range: 1.71 - 6.51, $p=0.16$, Fig. 4b) patients.

FMISO uptake volume

Uptake volume of FMISO was larger in GBM (27.18±10.46 %, range: 14.02 -

46.67 %) than in non-GBM (6.07±2.50 %, range: 2.12 - 9.22 %, $p<0.001$, Fig. 4b). The representative images of volume measurement process are shown in Fig. 6.

Discussion

Our results indicated that FMISO highly accumulated in all the GBM but not in the non-GBM gliomas. On the other hand, FDG accumulated in both GBM (100 %) and non-GBM gliomas (33 %), showing superior performance of FMISO PET relative to that of FDG PET in differential diagnosis. These results of visual analysis were supported by the analyses of SUV, lesion-to-normal tissue ratio, and FMISO uptake volume.

In the WHO definition, grade IV gliomas show microvascular proliferation and necrosis as well as anaplasia and mitotic activity [1]. On the other hand, necrotic tissues are not observed in grade III or lower grade gliomas. Therefore, necrotic change is one of the most important histopathological landmarks that distinguish GBM from lower grade gliomas. Furthermore, the necrosis in GBM is considered to be associated with tissue hypoxia [16, 17], which can be visualized using FMISO PET. Injected FMISO is first taken up by viable cells, and then oxidized and excreted by normoxic cells but

retained in hypoxic cells [37]. Therefore, we consider that FMISO accumulates in peri-necrotic hypoxic tissues, but not in the necrotic region exactly. Interestingly, we observed that FMISO highly accumulated in GBM lesions showing homogenous enhancement by gadolinium without a necrotic core described on MR images (Fig. 1, arrowhead). This finding suggested the possibility that even a microscopic necrosis may be surrounded by a hypoxic area sufficiently large to be identified by FMISO PET.

In this study, FMISO did not highly accumulate in non-GBM patients. Previous studies measured oxygen partial pressure in human gliomas directly using needle electrodes [18, 19, 38]. These papers reported that not only GBM but also grade II and III gliomas survived under hypoxic conditions. However, lower grade gliomas, which do not develop necrosis, showed milder hypoxia than that in GBM [18, 19]. In addition, FMISO accumulation requires severe hypoxia usually with oxygen partial pressure less than 10 mmHg [39, 40]. Our results are consistent with these lines of evidence.

FMISO uptake in various tumors in correlation with histological findings was previously investigated by Cher *et al* [26]. They reported that, while all grade IV tumors showed high FMISO uptake, all grade I and II tumors showed FMISO uptake comparable to surrounding tissues. They also observed slightly elevated FMISO uptake in 1 of 3 grade III patients but not in remaining 2 grade III patients. Our results are

consistent with the previous data, except for grade III patients. Major difference in methodology between these studies is uptake time. They conducted FMISO scanning 2 hours after injection, while we did 4 hours after. Although protocols with 2 hours as uptake time are often used for FMISO study, Thorwarth *et al*. expressed a concern about 2 hours imaging of FMISO [41]. Using kinetic analysis for dynamic dataset of FMISO PET, they demonstrated that some hot spots detected at 2 hours were not actually hypoxic, but rather reflected high initial influx of the tracer due to increased blood flow. In the current study, no grade III patients showed high FMISO uptake, possibly because relatively long uptake time allowed the tracer to be excreted from tissues without severe hypoxia. PET scanning 4 hours after FMISO injection might be favorable to discrimination of grade III from grade IV, although this is still inconclusive in the current study where the number of grade III patients is limited.

Noninvasive discrimination using FMISO may directly contribute to diagnosis in clinical settings. The new technique may suggest the possibility of avoiding biopsy or resection followed by pathological investigation. It will be particularly advantageous for aged patients or patients with impaired performance status, preventing the unfavorable effects of surgery.

It is well known that FDG uptake reflects the histological aggressiveness of

glioma, and therefore, GBM shows the highest FDG uptake among the gliomas [12-14]. In this study, high FDG uptake was unexceptionally observed in GBM patients, but at the same time, 3 of 9 non-GBM patients also showed high FDG uptake. These findings are consistent with previously published data [13, 14]. FDG PET is undoubtedly useful for histological grading but inconclusive when the differential diagnosis of GBM is crucial. We suggest that FMISO PET may play an important role particularly when the tumor shows FDG uptake equal to or greater than that in the gray matter.

We evaluated FMISO PET images in the different manners consisting of visual assessment, SUV, lesion-to-normal tissue ratio, and uptake volume. These analyses produced consistent results concerning the relationship between FMISO uptake and glioma grade. In the clinical settings, because these semi-quantitative values did not have additional information, a straightforward method of visual inspection may be enough for differential diagnosis. Although SUV_{max} and SUV_{10mm} of FMISO was higher in GBM patients than in non-GBM patients, the ranges of these values for each group showed overlapping. This may be explained by inter-subject variability of SUV as well as the different PET scanner used for 1 non-GBM patient (No. 23). In contrast, the lesion-to-cerebellum ratio clearly separated GBM patients from non-GBM patients. The usefulness of the lesion-to-cerebellum ratio was demonstrated by Bruehlmeier *et al* [25].

They showed that lesion-to-cerebellum ratio was comparable with distribution volume of FMISO. Although cerebral glioma patients often show asymmetric blood flow of the cerebellum (so called crossed cerebellar diaschisis), FMISO accumulation of left and right cerebellar cortex did not show significant asymmetry in the current study (data not shown). Our results may support the use of the lesion-to-cerebellum ratio instead of simple values of SUV_{max} or SUV_{10mm}.

To further confirm the findings, we measured uptake volume of FMISO in the tumor and compared it between GBM and non-GBM patients. GBM contained considerably larger uptake volume of FMISO than non-GBM did. The hypoxic volume is generally delineated according to a tissue/blood ratio ≥ 1.2 in the images acquired 2 hours after FMISO injection [27-30]. Since we did not collect blood sample at the scanning time, we did not apply this method. In brain tumor segmentation for ^{11}C methionine PET, a method of tumor/normal ratio ≥ 1.3 is frequently used [30, 35, 36]. Accordingly, we measured intratumoral volume showing higher accumulation than 1.3-fold cerebellum mean. Although we understand that this method did not directly quantify hypoxic volume, the results of this analysis were consistent to the results of visual and other semi-quantitative analyses, and therefore can reinforce our findings.

There are limitations in this study. First, the number of patients included in this

study was limited. Further study with more patients is necessary to reinforce our findings. In particular, small GBM lesions and aggressive grade III tumors should be focused on. Second, the current study did not investigate immunohistochemical features regarding hypoxia, such as hypoxia-inducible factor-1α. Finally, metastatic tumors and malignant lymphomas also require differential diagnosis from GBM. Future studies have to include various types of brain tumor and further clarify the clinical role of FMISO PET.

Conclusion

The preliminary study demonstrated that FMISO highly accumulated in GBM but not in non-GBM and that FMISO PET discriminated GBM from less malignant gliomas. FDG PET did not perfectly distinguish these entities in this study. Thus, although a larger study including more patients is necessary to support our findings, FMISO PET might be one of the useful tools for preoperative evaluation of cerebral glioma.

Acknowledgments

The authors would like to thank the staff of the Department of Nuclear Medicine, Central Institute of Isotope Science, and Department of Cancer Pathology, Hokkaido University, and Department of Radiology, Hokkaido University Hospital for supporting this work.

Conflict of Interest

This study was performed through Special Coordination Funds for Promoting Science and Technology of the Ministry of Education, Culture, Sports, Science and Technology of Japan. This research was also supported in part by a Grant-in-Aid for General Scientific Research from the Japan Society for the Promotion of Science.

References

1. Louis DN, Ohgaki H, Wiestler OD, Cavenee WK, Burger PC, Jouvet A, et al. The 2007 WHO classification of tumours of the central nervous system. Acta Neuropathol. 2007;114:97-109. doi:10.1007/s00401-007-0243-4.

2. Gorlia T, van den Bent MJ, Hegi ME, Mirimanoff RO, Weller M, Cairncross JG, et al. Nomograms for predicting survival of patients with newly diagnosed glioblastoma: prognostic factor analysis of EORTC and NCIC trial 26981-22981/CE.3. Lancet Oncol. 2008;9:29-38. doi:S1470-2045(07)70384-4 [pii] 10.1016/S1470-2045(07)70384-4.

3. Cho KH, Kim JY, Lee SH, Yoo H, Shin SH, Moon SH, et al. Simultaneous integrated boost intensity-modulated radiotherapy in patients with high-grade gliomas. Int J Radiat Oncol Biol Phys. 2010;78:390-7. doi:S0360-3016(09)02967-8 [pii] 10.1016/j.ijrobp.2009.08.029.

4. Behin A, Hoang-Xuan K, Carpentier AF, Delattre JY. Primary brain tumours in adults. Lancet. 2003;361:323-31. doi:S0140-6736(03)12328-8 [pii] 10.1016/S0140-6736(03)12328-8.

5. Spetzler RF, Martin NA. A proposed grading system for arteriovenous

malformations. J Neurosurg. 1986;65:476-83. doi:10.3171/jns.1986.65.4.0476.

6. Sawaya R. Extent of resection in malignant gliomas: a critical summary. J Neurooncol. 1999;42:303-5.

7. Stewart LA. Chemotherapy in adult high-grade glioma: a systematic review and meta-analysis of individual patient data from 12 randomised trials. Lancet. 2002;359:1011-8. doi:S0140673602080911 [pii].

8. Brasch R, Pham C, Shames D, Roberts T, van Dijke K, van Bruggen N, et al. Assessing tumor angiogenesis using macromolecular MR imaging contrast media. J Magn Reson Imaging. 1997;7:68-74.

9. Law M, Oh S, Babb JS, Wang E, Inglese M, Zagzag D, et al. Low-grade gliomas: dynamic susceptibility-weighted contrast-enhanced perfusion MR imaging--prediction of patient clinical response. Radiology. 2006;238:658-67. doi:2382042180 [pii]

10.1148/radiol.2382042180.

10. Cao Y, Nagesh V, Hamstra D, Tsien CI, Ross BD, Chenevert TL, et al. The extent and severity of vascular leakage as evidence of tumor aggressiveness in high-grade gliomas. Cancer Res. 2006;66:8912-7. doi:66/17/8912 [pii]

10.1158/0008-5472.CAN-05-4328.

11. Emblem KE, Nedregaard B, Nome T, Due-Tonnessen P, Hald JK, Scheie D, et al. Glioma grading by using histogram analysis of blood volume heterogeneity from MR-derived cerebral blood volume maps. Radiology. 2008;247:808-17. doi:247/3/808 [pii]

10.1148/radiol.2473070571.

12. Di Chiro G, DeLaPaz RL, Brooks RA, Sokoloff L, Kornblith PL, Smith BH, et al. Glucose utilization of cerebral gliomas measured by [18F] fluorodeoxyglucose and positron emission tomography. Neurology. 1982;32:1323-9.

13. Kaschten B, Stevenaert A, Sadzot B, Deprez M, Degueldre C, Del Fiore G, et al. Preoperative evaluation of 54 gliomas by PET with fluorine-18-fluorodeoxyglucose and/or carbon-11-methionine. J Nucl Med. 1998;39:778-85.

14. Padma MV, Said S, Jacobs M, Hwang DR, Dunigan K, Satter M, et al. Prediction of pathology and survival by FDG PET in gliomas. J Neurooncol. 2003;64:227-37.

15. Borbely K, Nyary I, Toth M, Ericson K, Gulyas B. Optimization of semi-quantification in metabolic PET studies with 18F-fluorodeoxyglucose and 11C-methionine in the determination of malignancy of gliomas. J Neurol Sci. 2006;246:85-94. doi:S0022-510X(06)00051-7 [pii]

10.1016/j.jns.2006.02.015.

16. Oliver L, Olivier C, Marhuenda FB, Campone M, Vallette FM. Hypoxia and the malignant glioma microenvironment: regulation and implications for therapy. Curr Mol Pharmacol. 2009;2:263-84.

17. Flynn JR, Wang L, Gillespie DL, Stoddard GJ, Reid JK, Owens J, et al. Hypoxia-regulated protein expression, patient characteristics, and preoperative imaging as predictors of survival in adults with glioblastoma multiforme. Cancer. 2008;113:1032-42. doi:10.1002/cncr.23678.

18. Evans SM, Judy KD, Dunphy I, Jenkins WT, Hwang WT, Nelson PT, et al. Hypoxia is important in the biology and aggression of human glial brain tumors. Clin Cancer Res. 2004;10:8177-84. doi:10/24/8177 [pii]

10.1158/1078-0432.CCR-04-1081.

19. Lally BE, Rockwell S, Fischer DB, Collingridge DR, Piepmeier JM, Knisely JP. The interactions of polarographic measurements of oxygen tension and histological grade in human glioma. Cancer J. 2006;12:461-6.

20. Rasey JS, Grunbaum Z, Magee S, Nelson NJ, Olive PL, Durand RE, et al. Characterization of radiolabeled fluoromisonidazole as a probe for hypoxic cells. Radiat Res. 1987;111:292-304.

21. Martin GV, Caldwell JH, Rasey JS, Grunbaum Z, Cerqueira M, Krohn KA. Enhanced binding of the hypoxic cell marker [3H]fluoromisonidazole in ischemic myocardium. J Nucl Med. 1989;30:194-201.

22. Rasey JS, Koh WJ, Grierson JR, Grunbaum Z, Krohn KA. Radiolabelled fluoromisonidazole as an imaging agent for tumor hypoxia. Int J Radiat Oncol Biol Phys. 1989;17:985-91.

23. Valk PE, Mathis CA, Prados MD, Gilbert JC, Budinger TF. Hypoxia in human gliomas: demonstration by PET with fluorine-18-fluoromisonidazole. J Nucl Med. 1992;33:2133-7.

24. Rajendran JG, Mankoff DA, O'Sullivan F, Peterson LM, Schwartz DL, Conrad EU, et al. Hypoxia and glucose metabolism in malignant tumors: evaluation by [18F]fluoromisonidazole and [18F]fluorodeoxyglucose positron emission tomography imaging. Clin Cancer Res. 2004;10:2245-52.

25. Bruehlmeier M, Roelcke U, Schubiger PA, Ametamey SM. Assessment of hypoxia and perfusion in human brain tumors using PET with 18F-fluoromisonidazole and 15O-H2O. J Nucl Med. 2004;45:1851-9. doi:45/11/1851 [pii].

26. Cher LM, Murone C, Lawrentschuk N, Ramdave S, Papenfuss A, Hannah A, et al. Correlation of hypoxic cell fraction and angiogenesis with glucose metabolic rate in

gliomas using 18F-fluoromisonidazole, 18F-FDG PET, and immunohistochemical studies. J Nucl Med. 2006;47:410-8. doi:47/3/410 [pii].

27. Spence AM, Muzi M, Swanson KR, O'Sullivan F, Rockhill JK, Rajendran JG, et al. Regional hypoxia in glioblastoma multiforme quantified with [18F]fluoromisonidazole positron emission tomography before radiotherapy: correlation with time to progression and survival. Clin Cancer Res. 2008;14:2623-30. doi:14/9/2623 [pii]
10.1158/1078-0432.CCR-07-4995.

28. Swanson KR, Chakraborty G, Wang CH, Rockne R, Harpold HL, Muzi M, et al. Complementary but distinct roles for MRI and 18F-fluoromisonidazole PET in the assessment of human glioblastomas. J Nucl Med. 2009;50:36-44. doi:jnumed.108.055467 [pii]
10.2967/jnumed.108.055467.

29. Szeto MD, Chakraborty G, Hadley J, Rockne R, Muzi M, Alvord EC, Jr., et al. Quantitative metrics of net proliferation and invasion link biological aggressiveness assessed by MRI with hypoxia assessed by FMISO-PET in newly diagnosed glioblastomas. Cancer Res. 2009;69:4502-9. doi:0008-5472.CAN-08-3884 [pii]
10.1158/0008-5472.CAN-08-3884.

30. Kawai N, Maeda Y, Kudomi N, Miyake K, Okada M, Yamamoto Y, et al. Correlation of biological aggressiveness assessed by 11C-methionine PET and hypoxic burden assessed by 18F-fluoromisonidazole PET in newly diagnosed glioblastoma. Eur J Nucl Med Mol Imaging. 2011;38:441-50. doi:10.1007/s00259-010-1645-4.

31. Oh SJ, Chi DY, Mosdzianowski C, Kim JY, Gil HS, Kang SH, et al. Fully automated synthesis of [18F]fluoromisonidazole using a conventional [18F]FDG module. Nucl Med Biol. 2005;32:899-905. doi:S0969-8051(05)00149-6 [pii]
10.1016/j.nucmedbio.2005.06.003.

32. Tang G, Wang M, Tang X, Gan M, Luo L. Fully automated one-pot synthesis of [18F]fluoromisonidazole. Nucl Med Biol. 2005;32:553-8. doi:S0969-8051(05)00080-6 [pii]
10.1016/j.nucmedbio.2005.03.010.

33. Minoshima S, Frey KA, Koeppe RA, Foster NL, Kuhl DE. A diagnostic approach in Alzheimer's disease using three-dimensional stereotactic surface projections of fluorine-18-FDG PET. J Nucl Med. 1995;36:1238-48.

34. Minoshima S, Koeppe RA, Frey KA, Kuhl DE. Anatomic standardization: linear scaling and nonlinear warping of functional brain images. J Nucl Med. 1994;35:1528-37.

35. Kracht LW, Miletic H, Busch S, Jacobs AH, Voges J, Hoevels M, et al. Delineation of brain tumor extent with [11C]L-methionine positron emission tomography: local comparison with stereotactic histopathology. Clin Cancer Res. 2004;10:7163-70. doi:10/21/7163 [pii]

10.1158/1078-0432.CCR-04-0262.

36. Galldiks N, Ullrich R, Schroeter M, Fink GR, Jacobs AH, Kracht LW. Volumetry of [(11)C]-methionine PET uptake and MRI contrast enhancement in patients with recurrent glioblastoma multiforme. Eur J Nucl Med Mol Imaging. 2010;37:84-92. doi:10.1007/s00259-009-1219-5.

37. Lee ST, Scott AM. Hypoxia positron emission tomography imaging with 18f-fluoromisonidazole. Semin Nucl Med. 2007;37:451-61. doi:S0001-2998(07)00084-0 [pii]

10.1053/j.semnuclmed.2007.07.001.

38. Collingridge DR, Piepmeier JM, Rockwell S, Knisely JP. Polarographic measurements of oxygen tension in human glioma and surrounding peritumoural brain tissue. Radiother Oncol. 1999;53:127-31. doi:S0167-8140(99)00121-8 [pii].

39. Koch CJ, Evans SM. Non-invasive PET and SPECT imaging of tissue hypoxia using isotopically labeled 2-nitroimidazoles. Adv Exp Med Biol. 2003;510:285-92.

40. Rasey JS, Nelson NJ, Chin L, Evans ML, Grunbaum Z. Characteristics of the binding of labeled fluoromisonidazole in cells in vitro. Radiat Res. 1990;122:301-8.

41. Thorwarth D, Eschmann SM, Paulsen F, Alber M. A kinetic model for dynamic [18F]-Fmiso PET data to analyse tumour hypoxia. Phys Med Biol. 2005;50:2209-24. doi:S0031-9155(05)90294-7 [pii]

10.1088/0031-9155/50/10/002.

Figure Captions

Fig. 1 A 64-year-old man (patient No. 2) presented with bilateral frontal lobe tumor on FLAIR MR imaging (a). Gadolinium-enhanced MR imaging revealed multiple lesions (b), one with ring-like enhancement (arrow) and another with homogenous enhancement (arrowhead). Both lesions showed FMISO uptake greater than that in surrounding brain tissues (c) (*high FMISO uptake*), and also FDG uptake greater than that in the cerebral cortex (d) (*high FDG uptake*). The histological diagnosis was glioblastoma multiforme

Fig. 2 A 34-year-old woman (patient No. 16) presented a tumor in the left frontal lobe shown on FLAIR MR imaging (a). A part of the tumor was strongly enhanced with gadolinium (b, arrow). The tumor showed FMISO uptake equal to that in surrounding brain tissues (c) (*intermediate FMISO uptake*), but showed FDG uptake greater than that in the cerebral cortex (d, arrow) (*high FDG uptake*). The histological diagnosis was anaplastic oligodendroglioma (grade III)

Fig. 3 A 44-year-old man (patient No. 23) presented a tumor in the left temporal lobe

revealed on FLAIR MR imaging (a). Weak gadolinium enhancement was observed in the tumor (b). The tumor showed FMISO uptake equal to surrounding brain tissues (c) (*intermediate FMISO uptake*), and showed FDG uptake greater than that in the white matter and less than that in the cerebral cortex (d) (*intermediate FDG uptake*). The histological diagnosis was oligodendroglioma (grade II)

Fig. 4 The lesion-to-cerebellum ratio of FMISO (a) was higher for GBM patients than for non-GBM patients ($p<0.001$). The uptake volume of FMISO (b) was larger for GBM patients than for non-GBM patients ($p<0.001$)

Fig. 5 The lesion-to-gray matter ratio of FDG (a) was higher for GBM patients than for non-GBM patients ($p<0.05$), whereas the lesion-to-white matter ratio of FDG (b) did not reach statistical significance ($p=0.16$). The diabetic patient (No. 13) was not plotted

Fig. 6 Measurement of FMISO uptake volume (patient No. 2 (a), and No. 23 (b)). The polygonal ROIs were manually drawn on every slice. The number of voxels showing higher values than mean of cerebellum was counted (red voxles)

Fig. 1

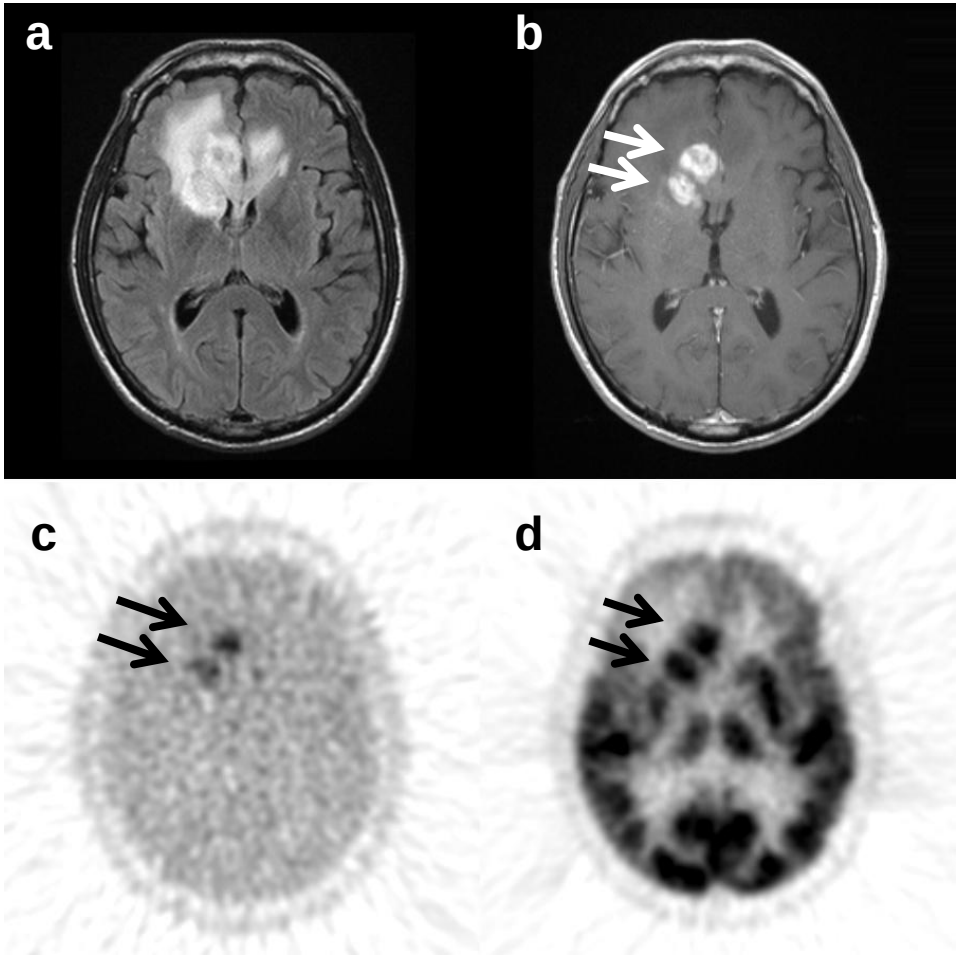

Fig. 2

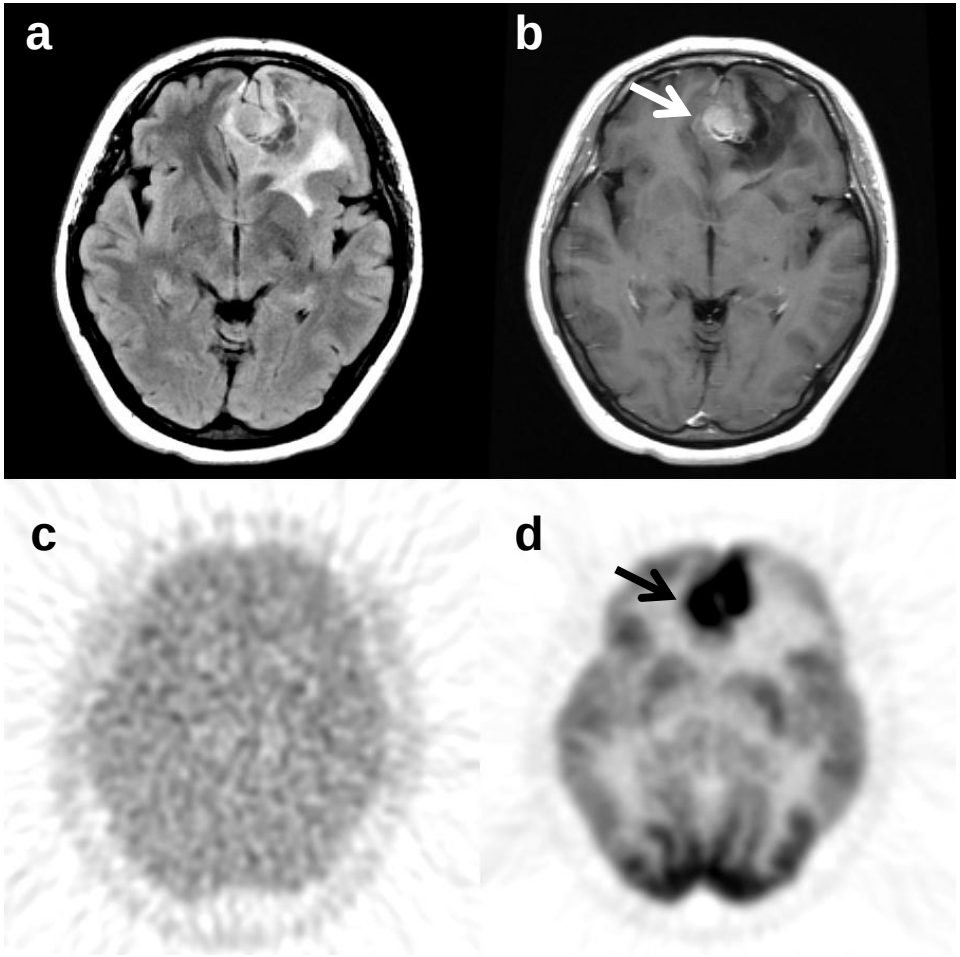

Fig. 3

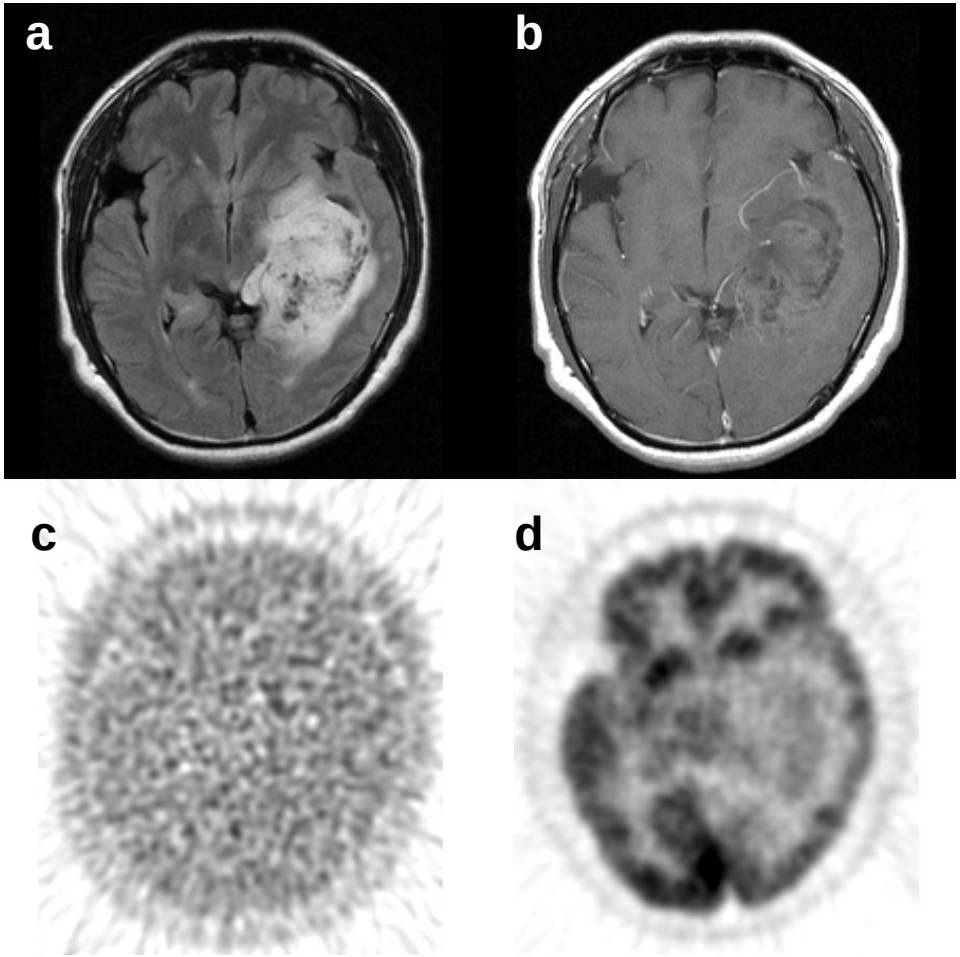

Fig. 4

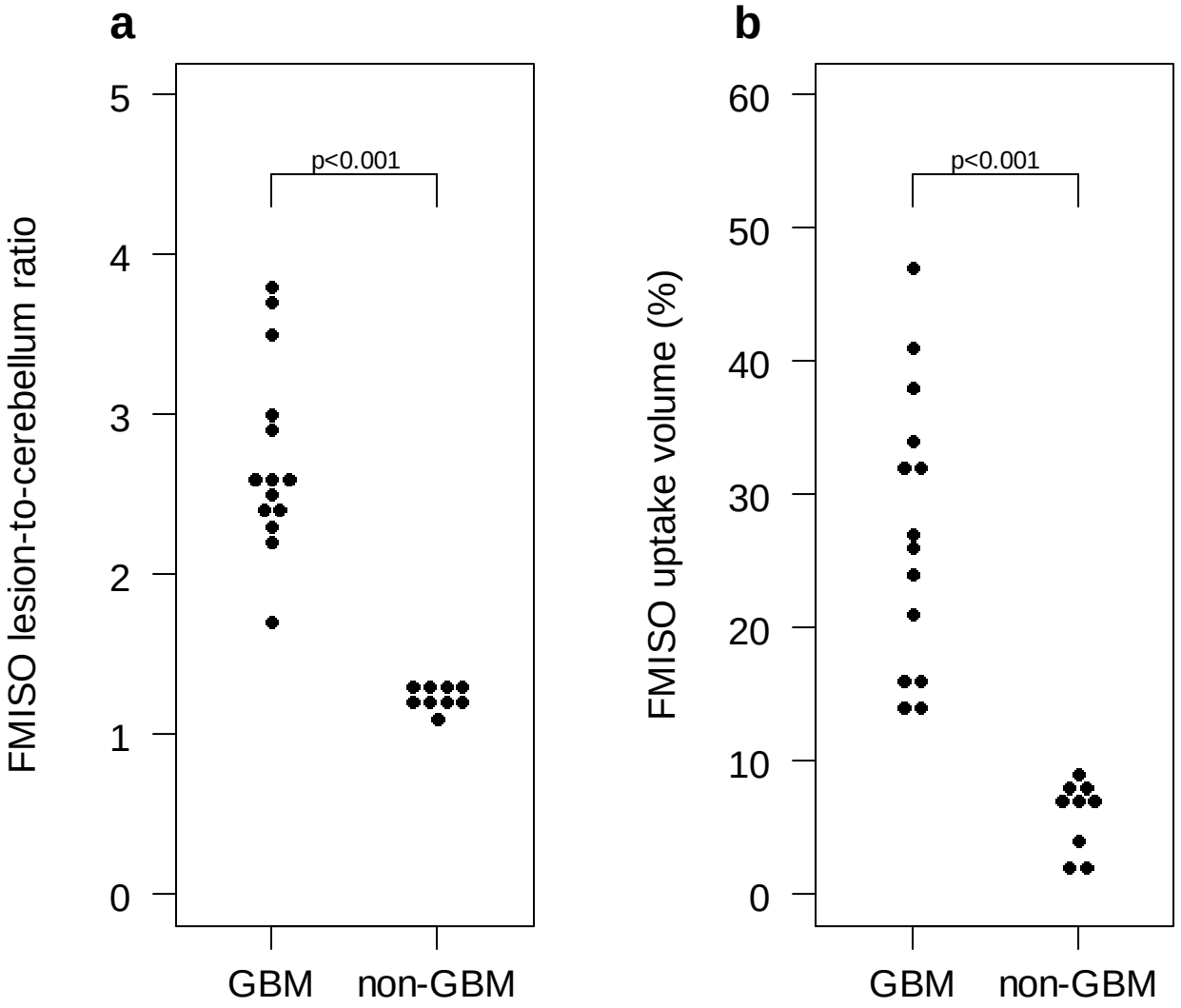
a
FMISO lesion-to-cerebellum ratio
5
4
3
2
1
0
p<0.001
GBM
non-GBM
b
FMISO uptake volume (%)
60
50
40
30
20
10
0
p<0.001
GBM
non-GBM

Fig. 5

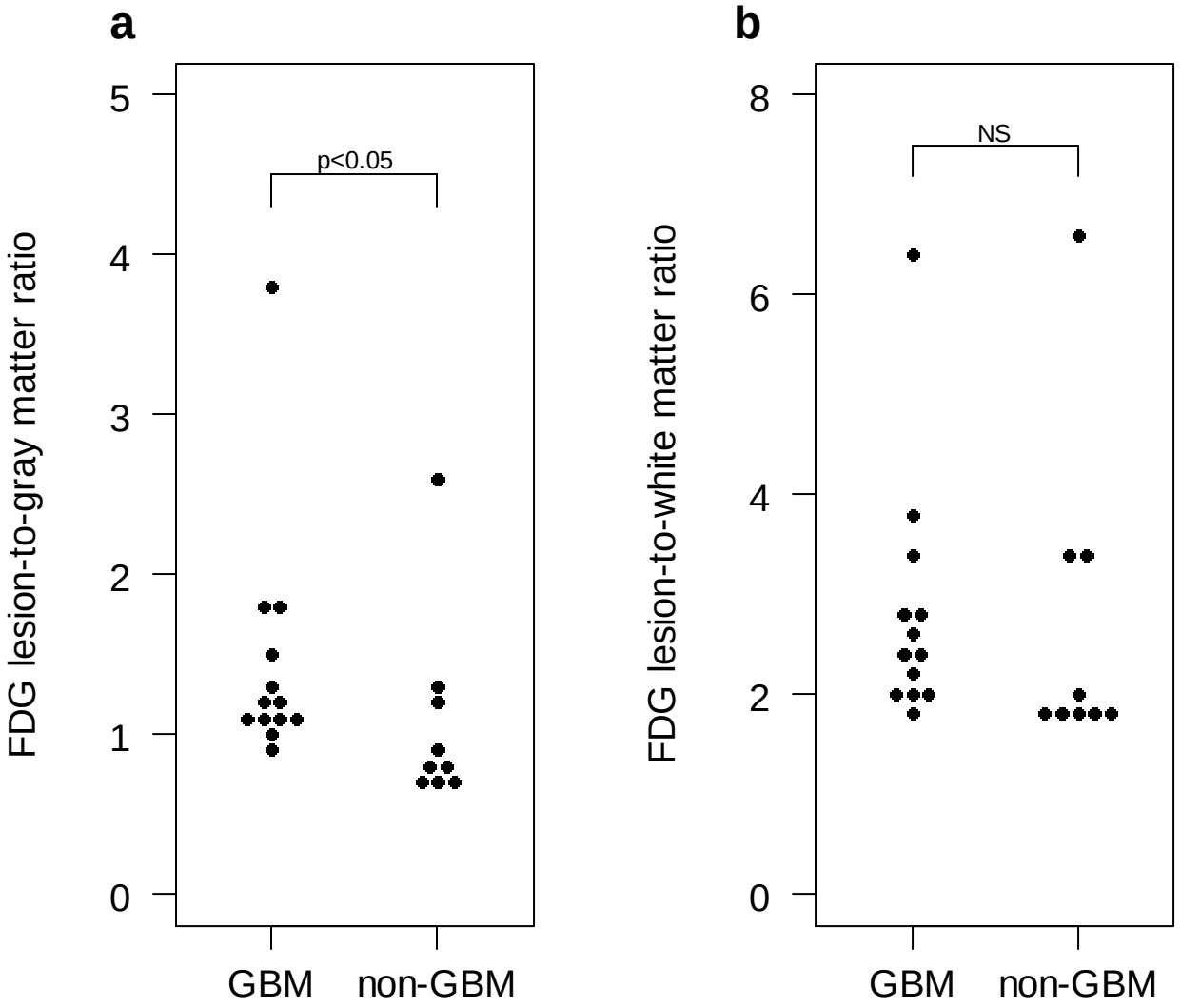
a
FDG lesion-to-gray matter ratio
p<0.05
GBM
non-GBM
b
FDG lesion-to-white matter ratio
NS
GBM
non-GBM

Fig. 6

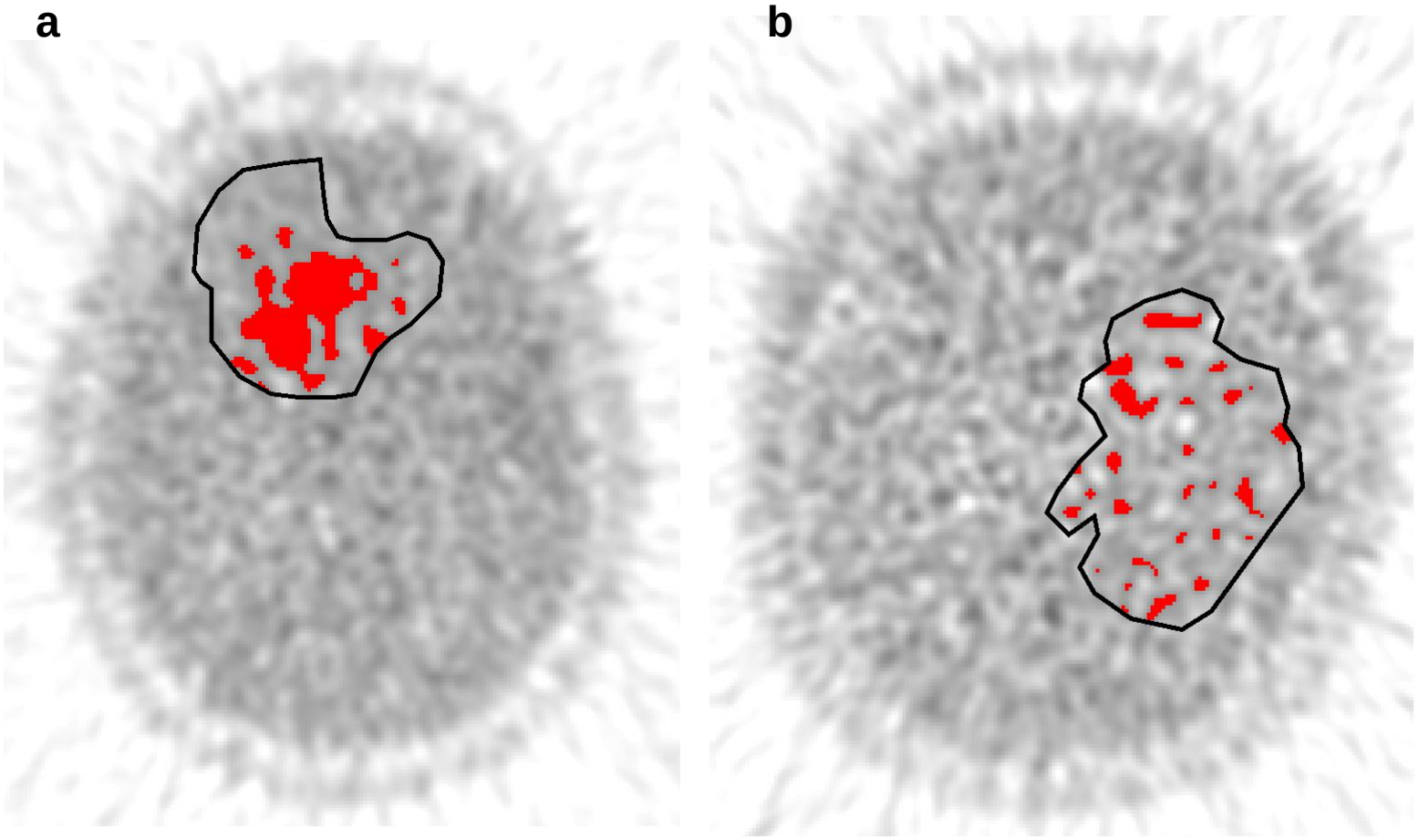

Table 1. Characteristics of 23 glioma patients

No.*	Age	Sex	WHO Grade	Histological Diagnosis	MRI Enhancement	Tumor Size (mm)	
						FLAIR	Enhancement
1	66	F	IV	GBM	strong	85.7	40.4
2	64	M	IV	GBM	strong	66.8	43.6
3	75	F	IV	GBM	strong	66.6	46.5
4	51	M	IV	GBM	strong	69.1	46.0
5	79	F	IV	GBM	strong	65.2	54.4
6	82	M	IV	GBM	strong	74.4	44.4
7	59	F	IV	GBM	strong	63.7	58.7
8	59	F	IV	GBM	strong	26.8	16.4
9	63	M	IV	GBM	strong	50.2	39.9
10	79	F	IV	GBM	strong	47.5	16.7
11	55	F	IV	GBM	strong	45.8	35.0
12	56	M	IV	GBM	strong	96.1	59.4
13	60	F	IV	GBM	strong	68.2	44.1
14	69	F	IV	GBM	strong	74.8	46.9
15	43	F	III	AA	weak	52.3	24.6
16	34	F	III	AO	strong	68.8	26.6
17	40	M	III	AOA	strong	62.6	48.9
18	31	M	III	AOA	absent	107.5	NA
19	64	M	III	AOA	strong	62.7	23.0
20	64	F	II	DA	absent	118.3	NA
21	37	M	II	OA	weak	85.8	37.9
22	36	F	II	OA	absent	61.5	NA
23	44	M	II	OD	weak	79.5	57.4

*Patient No. 15 was a recurrent case. AO = anaplastic oligodendroglioma; AOA = anaplastic oligoastrocytoma; GBM = glioblastoma multiforme; NA = not available; OA = oligoastrocytoma; OD = oligodendroglioma

Table 2. FMISO and FDG PET results

		FMISO					FDG				
No.*	WHO Grade	Visual Assessment	SUV_{max}	SUV_{10mm}	Lesion-to-cerebellum ratio	Uptake Volume (%)	Visual Assessment	SUV_{max}	SUV_{10mm}	Lesion-to-gray matter ratio	Lesion-to-white matter ratio
1	IV	High	2.79	2.69	2.33	14.02	High	6.48	6.37	0.91	2.10
2	IV	High	2.68	2.58	2.59	21.24	High	6.71	6.57	1.27	2.75
3	IV	High	3.46	3.40	2.63	24.11	High	4.39	4.32	1.49	2.33
4	IV	High	2.96	2.87	3.05	31.80	High	7.72	7.56	1.76	3.34
5	IV	High	3.41	3.35	3.70	34.33	High	4.34	4.26	1.11	1.87
6	IV	High	3.27	3.12	2.63	37.59	High	14.30	14.16	3.79	6.44
7	IV	High	2.22	2.15	2.23	41.04	High	6.47	6.34	1.11	2.41
8	IV	High	2.62	2.51	1.71	15.72	High	5.18	5.08	0.97	1.91
9	IV	High	2.94	2.83	2.35	14.15	High	16.38	15.90	1.85	3.82
10	IV	High	2.28	2.24	2.36	26.79	High	4.64	4.54	1.09	1.96
11	IV	High	4.31	4.18	3.48	46.67	High	6.19	6.11	1.15	2.15
12	IV	High	2.89	2.78	2.50	25.66	High	8.90	8.73	1.25	2.87
13	IV	High	4.19	4.11	3.81	31.62	(High)	(4.22)	(4.12)	(1.56)	(2.68)
14	IV	High	3.27	3.19	2.93	15.81	High	6.46	6.41	1.18	2.63
15	III	Int	1.38	1.30	1.19	6.64	Int	5.39	5.22	0.66	1.73
16	III	Int	2.02	1.91	1.29	7.72	High	23.49	23.12	2.59	6.51
17	III	Int	1.62	1.52	1.27	7.62	High	9.36	9.18	1.29	3.37
18	III	Int	1.42	1.29	1.09	7.31	Int	4.75	4.64	0.75	1.73
19	III	Int	1.36	1.29	1.16	2.47	Low	5.40	5.24	0.88	2.02
20	II	Int	1.87	1.76	1.26	4.30	Low	4.89	4.78	0.71	1.71
21	II	Int	1.51	1.39	1.21	9.22	High	9.75	9.48	1.25	3.33
22	II	Int	2.02	1.97	1.26	2.12	Low	5.59	5.44	0.69	1.72
23	II	Int	2.39	2.35	1.25	7.21	Int	5.29	5.16	0.81	1.79

*Patient No. 13 was excluded from the analysis of FDG PET because of hyperglycemia. FMISO images of patient No. 23 were acquired using Biograph 64 PET-CT. Int = Intermediate